



Technical note: Uncertainties in eddy covariance CO₂ fluxes in a semiarid sagebrush ecosystem caused by gap-filling approaches

Jingyu Yao¹, Zhongming Gao^{2,3}, Jianping Huang⁴, Heping Liu², and Guoyin Wang⁵

¹Key Laboratory for Semi-Arid Climate Change of the Ministry of Education, College of Atmospheric Sciences, Lanzhou University, Lanzhou, China

²Laboratory for Atmospheric Research, Department of Civil and Environmental Engineering, Washington State University, Pullman, Washington, USA

³School of Atmospheric Sciences, Sun Yat-sen University, Southern Marine Science and Engineering Guangdong Laboratory (Zhuhai), Zhuhai, China

⁴Collaborative Innovation Center for Western Ecological Safety, Lanzhou University, Lanzhou, China

⁵Department of Atmospheric and Oceanic Sciences & Institute of Atmospheric Sciences, Fudan University, Shanghai, China

Correspondence: Jianping Huang (hjp@lzu.edu.cn)

Received: 26 July 2021 – Discussion started: 28 July 2021

Revised: 23 September 2021 – Accepted: 25 September 2021 – Published: 18 October 2021

Abstract. Gap-filling eddy covariance CO₂ fluxes is challenging at dryland sites due to small CO₂ fluxes. Here, four machine learning (ML) algorithms including artificial neural network (ANN), *k*-nearest neighbors (KNNs), random forest (RF), and support vector machine (SVM) are employed and evaluated for gap-filling CO₂ fluxes over a semiarid sagebrush ecosystem with different lengths of artificial gaps. The ANN and RF algorithms outperform the KNN and SVM in filling gaps ranging from hours to days, with the RF being more time efficient than the ANN. Performances of the ANN and RF are largely degraded for extremely long gaps of 2 months. In addition, our results suggest that there is no need to fill the daytime and nighttime net ecosystem exchange (NEE) gaps separately when using the ANN and RF. With the ANN and RF, the gap-filling-induced uncertainties in the annual NEE at this site are estimated to be within 16 g C m⁻², whereas the uncertainties by the KNN and SVM can be as large as 27 g C m⁻². To better fill extremely long gaps of a few months, we test a two-layer gap-filling framework based on the RF. With this framework, the model performance is improved significantly, especially for the nighttime data. Therefore, this approach provides an alternative in filling extremely long gaps to characterize annual carbon budgets and interannual variability in dryland ecosystems.

1 Introduction

The eddy covariance (EC) technique has been widely applied for monitoring energy and water fluxes as well as net ecosystem exchanges (NEEs) of carbon dioxide and other trace gases between land and the atmosphere (Baldocchi, 2003; Oncley et al., 2007; Stoy et al., 2013). However, due to multiple factors including power outages, instrument malfunctions and maintenance, and data quality checks, there exist gaps with approximately 20 %–60 % of half-hourly data points annually at many long-term EC sites (Dragoni et al., 2007; Falge et al., 2001; Ma et al., 2007; Missik et al., 2019, 2021; Moffat et al., 2007; Pastorello et al., 2020; Soloway et al., 2017; Wutzler et al., 2018). An average gap fraction of 30 % in an annual dataset leads to an uncertainty of ±25 g C m⁻² yr⁻¹ for the annual NEE at forest sites (Moffat et al., 2007), while some EC sites report much greater uncertainties (Soloway et al., 2017). Therefore, gap-filling usually accounts for one large source of uncertainties in the annual NEE (Soloway et al., 2017), together with other sources of uncertainties such as measurement errors and bias related to non-closure of the surface energy balance (Gao et al., 2019; Wilson et al., 2002).

Robust NEE gap-filling approaches are critical for quantifying the annual and interannual variability of carbon budgets (Falge et al., 2001; Irvin et al., 2021; Moffat et al.,

2007; Pastorello et al., 2020; Richardson and Hollinger, 2007; Soloway et al., 2017; Wutzler et al., 2018). Previous studies have developed and evaluated a number of NEE gap-filling approaches including non-linear regressions (NLRs), look-up tables (e.g., marginal distribution sampling, MDS), machine learning (ML) algorithms (e.g., artificial neural networks), and process-based models (Falge et al., 2001; Huang and Hsieh, 2020; Moffat et al., 2007; Reichstein et al., 2005; Wutzler et al., 2018). NLR fills NEE gaps based on regression analyses between NEE and meteorological variables such as temperature (e.g., air or soil temperature) and light (e.g., photosynthetically active radiation), whereas MDS is based on look-up tables for similar meteorological conditions (i.e., global radiation, air temperature, and vapor pressure deficit) (Falge et al., 2001; Moffat et al., 2007; Reichstein et al., 2005). By virtue of an easy-to-use R package (Wutzler et al., 2018), MDS has become the standard method for NEE gap-filling (e.g., Pastorello et al., 2020), although it cannot effectively fill the gaps of longer than 12 d (Moffat et al., 2007). ML-based methods are trained by presenting them with numerous meteorological variables as inputs and NEE as output data, which have the potential to fill long gaps (Dengel et al., 2013; Kim et al., 2020; Moffat et al., 2007). Artificial neural networks (ANNs), for instance, have been widely used for gap-filling CO₂ and CH₄ fluxes across a variety of EC sites at forests, grasslands, croplands, and wetlands (Dengel et al., 2013; Delwiche et al., 2021; Huang and Hsieh, 2020; Irvin et al., 2021; Kim et al., 2020; Knox et al., 2016; Mahabbati et al., 2021; Moffat et al., 2007; Papale and Valentini, 2003; Soloway et al., 2017). More recently, other ML algorithms such as random forest (RF), *k*-nearest neighbors (KNNs), and support vector machine (SVM) have recently been assessed for flux gap-filling over different ecosystems, and RF is found to have outperformed the other ML algorithms as well as the MDS method (Huang and Hsieh, 2020; Irvin et al., 2021; Kim et al., 2020; Mahabbati et al., 2021). However, the performance of these ML-based algorithms has not been evaluated in filling gaps in EC fluxes for dryland ecosystems with low NEE.

Besides the selection of gap-filling algorithms, several other factors may also degrade the performance of the algorithms and cause uncertainties in gap-filled fluxes. For example, the performance of gap-filling algorithms decreases with increasing gap length (Huang and Hsieh, 2020; Irvin et al., 2021; Kim et al., 2020), and thus long gaps in CO₂ flux are considered one of the primary uncertainty sources of NEE estimation (Aubinet et al., 2012). In addition, spatial variability of CO₂ flux and meteorological drivers (e.g., soil temperature) due to heterogeneous landscapes around flux towers (Chu et al., 2021; Stoy et al., 2013) can lead to unknown bias in modeling research (Metzger, 2018). That is, the trained ML algorithms using the measured CO₂ flux and meteorological variables may not well reflect their real relationship within flux footprints and induce bias to gap-filled fluxes and the annual NEE.

Dryland ecosystems, comprising around 40 % of the Earth's land surface, play a critical role in determining the trend and interannual variability of the global terrestrial carbon budgets (Ahlström et al., 2015; Missik et al., 2021; Yao et al., 2020), though the expansion of projected global drylands under climate change is still under debate (Berg and McColl, 2021; Feng and Fu, 2013; Huang et al., 2016; Yao et al., 2020). Long-term continuous measurements of land surface fluxes over dryland ecosystems are critical for assessing the impact of climate change on the dryland carbon cycle (Missik et al., 2021; Yao et al., 2020). The motivation of this gap-filling practice was driven by the fact that dryland ecosystems are very sensitive to water availability, functioning as carbon sinks in wet years and carbon sources in dry years (Biederman et al., 2017; Scott et al., 2015), and bias in gap-filled NEE may alter conclusions in sources or sinks of dryland ecosystems in the case of relatively long gaps for eddy covariance data. In addition, different ML algorithms have distinctive internal structures that account for the underlying dependencies of outputs (i.e., NEE) on the inputs (i.e., meteorological variables) in different ways, and uncertainties associated with different ML-based methods can also be assessed (Soloway et al., 2017).

In this study, we evaluate the performance of four commonly used ML algorithms (ANN, KNN, RF, and SVM) in filling the extremely long gaps (i.e., couple months) in the NEE data collected at an EC site over a semiarid sagebrush ecosystem in central Washington, USA, from 2016 to 2019, and we assess the uncertainties in the annual NEE introduced by gap-filling methods. In order to fill the extremely long gaps, we propose and examine a two-layer RF-based gap-filling framework (RF-2L) as the RF benefits from better performance and faster run-time than the other ML algorithms (Huang and Hsieh, 2020; Irvin et al., 2021; Kim et al., 2020; Mahabbati et al., 2021).

2 Materials and methods

In this section, we first describe the site condition and instruments, as well as the procedures for EC data processing, quality control, and gap identification, following the standard protocol (Mauder and Foken, 2004). We then briefly introduce the four ML algorithms and the proposed framework of RF-2L, as well as the input meteorological variables. Following the previous studies (Moffat et al., 2007; Kim et al., 2020), four different lengths of artificial gaps are generated and used to evaluate the performance of these four ML algorithms, whereas the performance of RF-2L is evaluated with gaps of 2 months. We also examine the performance of the algorithms for different time-of-day scenarios: (1) all the data, (2) daytime data, and (3) nighttime data. Finally, uncertainties in monthly and annual NEE are quantified by comparing with the results from the MDS method and the ensemble mean of predictions of the ML algorithms.

2.1 Site description

The eddy covariance flux tower is located at the Hanford Site in the US state of Washington (AmeriFlux site: US-Hn1; 46°24′32″ N, 119°16′30″ W), and it started to collect data in December 2015 (Gao et al., 2019, 2020a, b; Missik et al., 2019). This semiarid site is predominantly covered by scattered shrubs and short grasses. Shrub species include *Artemisia tridentata* and *Chrysothamnus viscidiflorus*, and grasses include invasive weedy species (i.e., *Bromus tectorum* and *Salsola kali*) and native grasses (i.e., *Poa secunda*, *Pseudoroegneria spicata*, and *Stipa comata*) (Missik et al., 2019). The long-term (1986–2015) mean annual precipitation was 197 mm (varied between 100 and 300 mm for dry and wet years), most of which occurred late in the fall and early in winter (Missik et al., 2019). The soil texture in the top layer of 30 cm is loamy sand with small rocks and gravel interspersed (Gao et al., 2017; Missik et al., 2019). In this study, the 4-year data from 2016 to 2019 are analyzed. Annual precipitation in these 4 years was 217, 242, 169, and 210 mm, respectively; and mean annual air temperature was 12.9, 11.4, 12.7, and 11.2 °C, respectively (Missik et al., 2021).

2.2 Eddy covariance and meteorological measurements

The EC system included a three-dimensional sonic anemometer (CSAT3, Campbell Scientific, Inc.) and an open-path gas analyzer (LI-7500A, LI-COR, Inc.), and the EC data were sampled at a rate of 10 Hz. In addition, a variety of microclimate data were measured, including four-component radiation, air temperature and relative humidity, wind speed and direction, precipitation, soil heat flux, soil temperature, and volumetric water content (Gao et al., 2017, 2019, 2020a; Missik et al., 2019). These data were sampled at a rate of 1 Hz and stored as 30 min averages. Further, 15 min meteorological data from two weather stations close to the tower site were obtained from the Washington State University AgWeatherNet (AWN; <https://weather.wsu.edu/>, last access: 13 July 2020). The two AWN stations are located within 8 km of the tower. The 15 min data were averaged to half-hourly values to fill gaps in the tower meteorological data of global radiation (R_g), air temperature (T_{air}) and relative humidity (RH), vapor pressure deficit (VPD), wind speed (WS), precipitation (P), and soil temperature (T_{soil}). Thus, these half-hourly meteorological data for the study period are gap-free.

2.3 EC data processing, quality control, and gap identification

Raw 10 Hz EC data were processed using the EddyPro[®] software (version 7.06, LI-COR Biosciences, USA) to calculate the 30 min average fluxes of CO₂ (NEE) and latent (LE) and sensible (H) heat. The data were despiked and filtered for

physically impossible values and abnormal diagnostic values of the sonic anemometer and the gas analyzer. The double rotation method was applied to the sonic anemometer data. Block averaging was used to determine the turbulent fluctuations for each 30 min interval. The fluxes were corrected for the effects of high- and low-pass filtering (Massman, 2000, 2001; Moncrieff et al., 2004) and air density fluctuations (Webb et al., 1980). The corrected fluxes were quality checked according to Mauder and Foken (2004). After quality checking, the “REddyProc” R package (Wutzler et al., 2018) was used to determine the friction velocity (u_*) threshold, and NEE data with low-turbulence conditions were removed from the dataset.

For simplicity, we assigned a gap score of 2 to gaps due to field operations (e.g., instrument maintenance), electrical and/or instrument failures, a gap score of 1 to gaps due to low data quality (i.e., quality control and u_* filtering), and a score of 0 to flux data with good quality. Only the data with the score of 0 were used to train/test the gap-filling algorithms. Note that, for the data gaps with a score of 1, meteorological data from the flux tower were still available for NEE gap-filling, whereas for the data gaps with a score of 2, meteorological data from the flux tower also had gaps, and the data obtained from the two nearby AWN stations are thus used for gap-filling.

2.4 Machine learning algorithms

Four ML algorithms including the ANN, KNN, RF, and SVM were employed and evaluated for filling NEE gaps. In the following sections, we briefly describe the characteristics and implementation of each ML algorithm. The required parameters in each algorithm (e.g., the number of nodes in each hidden layer for the ANN; k value for the KNN) are optimized using the “caret” R package (Kuhn et al., 2020) with a 10-fold cross-validation repeated 10 times.

2.4.1 Artificial neural network (ANN)

The ANN algorithm has been successfully applied for filling NEE gaps in various ecosystems (Baldocchi and Sturtevant, 2015; Knox et al., 2016; Moffat et al., 2007; Papale and Valentini, 2003; Tramontana et al., 2016). In this study, we employed the “neuralnet” R package (Günther and Fritsch, 2010), the resilient back-propagation algorithm that has proven to be capable of gap-filling flux data (Dengel et al., 2013; Jammet et al., 2015; Kim et al., 2020; Knox et al., 2016). The required parameters for the ANN algorithm include the number of hidden layers and the number of nodes in each layer. Here, based on the parameter tuning results, we use two hidden layers with 12 and 10 nodes in the first and second hidden layers. We train the neural network 1000 times, and the mean prediction results of the top 20 runs based on their training and testing R^2 values are used to

fill NEE gaps (Baldocchi and Sturtevant, 2015; Knox et al., 2016).

2.4.2 *K*-nearest neighbors (KNNs)

The KNN algorithm (Fix and Hodges, 1951) is a non-parametric ML approach and has been used in many applications. For example, Chen et al. (2012) applied the KNN algorithm for filling latent heat flux gaps, which fills the data gaps based on a certain attribution of *k* neighbors in the feature space. In this study, we use the caret R package (Kuhn et al., 2020) to build the KNN where a suitable *k* value needs to be determined. Here, the optimized *k* value is 9.

2.4.3 Random forest (RF)

The RF algorithm (Breiman, 2001) has been applied for up-scaling flux data to regional (Xu et al., 2018) and global (Jung et al., 2017; Zeng et al., 2020) scales and recently for gap-filling flux data (Huang and Hsieh, 2020; Kim et al., 2020). The RF algorithm uses bootstrap aggregation and feature randomness when generating each individual tree to try to create many independent decision trees that operate as an ensemble of the prediction results. In this study, we create 500 regression trees for each case using the “randomForest” R package (Liaw and Wiener, 2002), in which the tuning parameter is the number of randomly selected predictors (i.e., *mtry* equals 7). In addition, the RF allows the estimation of relative importance of input variables, and such a feature has been utilized in previous studies to help interpret the results (Irvin et al. 2021; Kim et al., 2020).

2.4.4 Support vector machine (SVM)

The SVM algorithm (Cortes and Vapnik, 1995) has also been applied for gap-filling (Huang and Hsieh, 2020; Kim et al., 2020) and upscaling (Xu et al., 2018) flux data. The SVM algorithm can convert nonlinear regressions into linear regressions by projecting the original finite-dimensional space into the much higher-dimensional space with a predefined kernel function. In this study, we use the radial basic kernel function and the “kernlab” R package (Karatzoglou et al., 2004), where the tuning parameters include the inverse kernel width (i.e., $\sigma = 0.13$) and the cost regularization parameter (i.e., $C = 27$).

2.4.5 A two-layer RF-based gap-filling framework (RF-2L) for extremely long gaps

Numerous studies have suggested that the performance of ML algorithms decreases with increasing the gap length and that the ML algorithms are only reliable for gaps shorter than a couple weeks (Huang and Hsieh, 2020; Irvin et al., 2021; Kim et al., 2020; Mahabbati et al., 2021). In order to fill the extremely long gaps (i.e., a couple months), we propose and examine a two-layer RF-based gap-filling framework (RF-

2L) because the RF outperforms most of the other ML algorithms in gap-filling the half-hourly fluxes over various ecosystems (Huang and Hsieh, 2020; Irvin et al., 2021; Kim et al., 2020; Mahabbati et al., 2021) and is more time efficient than the ANN (Irvin et al., 2021). The procedures of the RF-2L include the following: (1) train the RF model using the half-hourly data and fill the NEE gaps shorter than 7 d; (2) calculate daily means of the input variables and the partially filled NEE data; and (3) train the RF model using the daily data and fill the gaps in the daily NEE data.

2.5 Input variables

Besides the abovementioned meteorological variables, the input variables for the ML algorithms also include the normalized difference vegetation index (NDVI) and enhanced vegetation index (EVI) from the Moderate Resolution Imaging Spectroradiometer (MODIS) and three fuzzy variables (i.e., decimal day of year and sine and cosine functions to represent seasonal changes) following Moffat et al. (2007). We obtained the NDVI and EVI data around the flux tower location from the MOD13Q1 version 6 data product (<https://lpdaac.usgs.gov/products/mod13q1v006/>, last access: 13 July 2020) at 16 d temporal and 250 m spatial resolutions (Didan, 2015). The 16 d NDVI and EVI data were resampled to 30 min using cubic spline interpolation. Note that soil water content (SWC) and groundwater table are not included in the inputs because (1) the SWC measurements at these AWN stations had some issues for the study period and could not be used to fill the long gaps in tower SWC data, and (2) the station is primarily fed by rainfall without groundwater access (Missik et al., 2019, 2021).

With the RF, we estimate the relative importance of the input variables for the three different time-of-day scenarios, respectively (Fig. 1). For the model trained using all the data and the daytime data, R_g is the most important variable, while for the model trained using the nighttime data, T_{air} and RH are the most important variables. Overall, the estimated variable importance indicates that, for the three different time-of-day scenarios, the meteorological inputs except R_g for the nighttime data play a comparable role in the trained gap-filling models. Note that there exists collinearity among the various variables, and thus the model performance might approach a plateau with certain input variables and increase slightly with increasing number of inputs, resulting in a slower, less efficient model. However, to be consistent with previous studies (e.g., Kim et al., 2020; Moffat et al., 2007), we also include all available meteorological variables as the inputs to train and evaluate the models.

2.6 Artificial gap scenarios and performance evaluation

In order to evaluate the gap-filling algorithms, artificial gaps with different lengths are randomly generated in the origi-

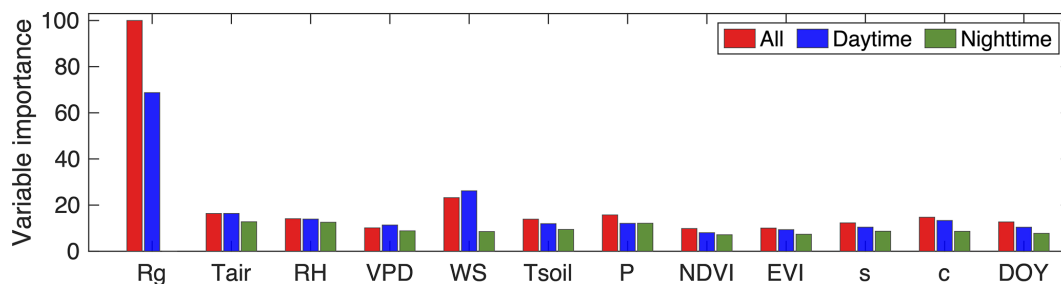


Figure 1. Variable importance for the random forest trained without separating the daytime and nighttime data (All) and separately for daytime and nighttime data. The variables DOY, *c*, and *s* indicate decimal day of year and cosine and sine functions, respectively.

nal flux data, accounting for approximately 10 %–12 % of the NEE data with a score of 0. Following Moffat et al. (2007) and Kim et al. (2020), we consider four artificial gap lengths: 1 h (1-H), 1 d (1-D), 1 week (1-W), and 2 months (2-M). The variations in the number of data points artificially removed are because after quality control it is hard to locate even a couple days of data without any missing points (Sect. 3.1). In order to reduce the potential effect of uneven sample sizes and gap positions on the performance evaluation, each gap length scenario is permuted 10 times, resulting in 40 distinct time series with artificial gap scenarios.

For each artificial gap scenario, we trained the models separately with only daytime or nighttime data and with both daytime and nighttime data. The performance of gap-filling algorithms is evaluated by comparing the estimated values (e_i) with the measured values (m_i) for the artificial gaps. Four commonly used performance metrics are used including the coefficient of determination (R^2), root-mean-square error (RMSE), mean absolute error (MAE), and bias error (BE).

$$R^2 = \frac{(\sum_{i=1}^n (e_i - \bar{e})(m_i - \bar{m}))^2}{\sum_{i=1}^n (e_i - \bar{e})^2 \sum_{i=1}^n (m_i - \bar{m})^2} \quad (1)$$

$$\text{RMSE} = \sqrt{\frac{\sum_{i=1}^n (e_i - m_i)^2}{\sum_{i=1}^n 1^n (m_i)^2}} \quad (2)$$

$$\text{MAE} = \frac{1}{n} \sum_{i=1}^n |e_i - m_i| \quad (3)$$

$$\text{BE} = \frac{1}{n} \sum_{i=1}^n (e_i - m_i) \quad (4)$$

Here the overbar denotes the mean value.

Besides the above statistic metrics, we also calculate the probability density functions of the measured and estimated values to examine the performance of ML algorithms in terms of different ranges of NEE values. Here, the probability density functions are calculated as the binned density

distribution of measured (estimated) NEE values divided by the bin width ($0.2 \mu\text{mol m}^{-2} \text{s}^{-1}$).

Previous studies also suggested that the model errors of gap-filling algorithms should approach the measurement random errors of the EC method (Kim et al., 2020; Moffat et al., 2007; Richardson et al., 2008). In this study, we compare the model errors with the random measurement errors as a reference. Here, the random measurement error is estimated following the method proposed by Finkelstein and Sims (2001).

2.7 Uncertainty estimation

With the 40 distinct artificial gap scenarios, we obtain 40 gap-filled NEE time series for each method. By replacing the artificial gaps with the observed data, these time series datasets allow for an evaluation of the model self-agreement and reliability in filling the actual gaps. Monthly and annual NEEs are then computed from the gap-filled flux time series. The model self-agreement can be evaluated by investigating the mean standard deviations of the monthly NEE (Soloway et al., 2017), whereas the uncertainties in the monthly and annual NEE can be assessed by comparing the monthly and annual NEE obtained by each ML algorithm with their ensemble means (Irvin et al., 2021; Kim et al., 2020; Soloway et al., 2017). Here, the flux time series gap-filled separately for the daytime and nighttime periods are combined to determine the monthly and annual NEEs.

3 Results

3.1 NEE data gap evaluation

At the US-Hn1 site, different lengths of gaps were found in NEE data during the 4 years from 2016 to 2019 (Fig. 2). Gaps with short to medium lengths were usually caused by low data quality (i.e., gap score of 1), whereas gaps with medium to extremely long lengths were mostly due to electrical and/or instrument failures (i.e., gap score of 2). Data gaps with a score of 1 frequently occurred in nighttime because u_* filtering mainly removes nighttime data. On average, gaps with scores of 1 and 2 accounted for about 28.4 % and 30.2 %

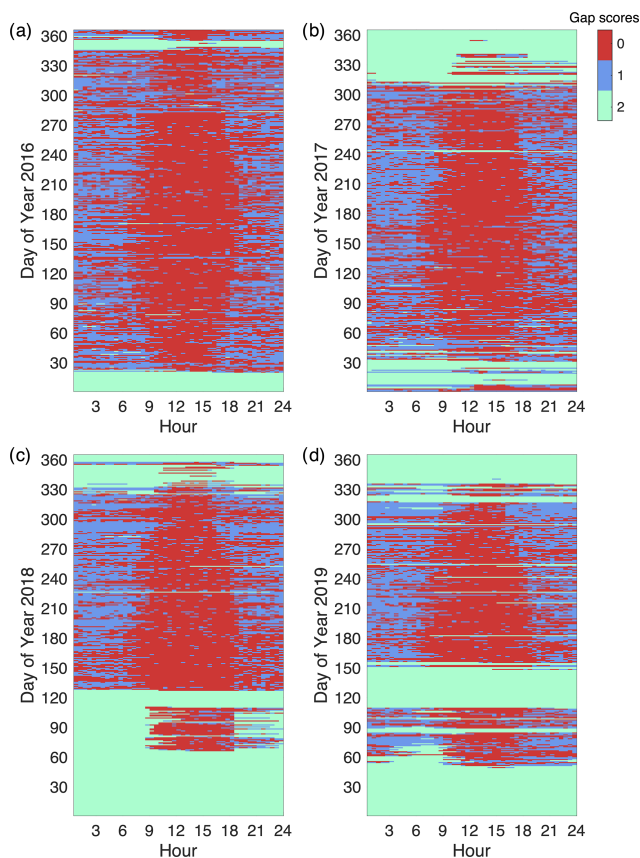


Figure 2. Distribution of NEE data gaps by day and hour from 2016 to 2019. NEE data gaps were classified as non-gaps (gap score: 0), gaps due to low data quality (gap score: 1), and gaps due to electrical and/or instrument failures (gap score: 2).

of half-hour NEE data, respectively (Table 1). There were more extremely long gaps in 2018 and 2019 than 2016 and 2017 due to power failures in winter and early spring. Therefore, it is worth examining the performances of gap-filling algorithms in filling different lengths of gaps. Overall, about 43.7 % of NEE data were available to calibrate and validate the gap-filling methods.

3.2 Performance of ML gap-filling algorithms with different gap lengths

We first train and evaluate the ML algorithms without separating the daytime and nighttime data (i.e., using all the data). The overall performance of each algorithm degrades as the gap length increases, while the RF slightly outperforms the other algorithms for all the gap scenarios (Fig. 3 and Table 2). For the gap length of 1 h (1-H), all four ML algorithms have the highest R^2 and the lowest RMSE and MAE. As the gap length increases, R^2 for all ML algorithms decreases and RMSE (MAE) increases. For 1-H, the RF has R^2 and RMSE of 0.77 ± 0.02 and 0.47 ± 0.02 , respectively, whereas for the gap length of 2 months (2-M), the R^2 decreases to 0.60 ± 0.22

and RMSE increases to 0.62 ± 0.17 , respectively. The magnitudes of BE for all ML algorithms also increase with the increasing gap lengths. The performance of these ML algorithms in NEE gap-filling at this semiarid sagebrush site is comparable to that at some grassland sites (Huang and Hsieh, 2020), but lower than that at forest and cropland sites (Huang and Hsieh, 2020; Moffat et al., 2007). The relatively low performance might be caused by the spatial complexities of the targeted CO₂ flux and input meteorological drivers within the flux footprints (Chu et al., 2021; Stoy et al., 2013), especially for the scattered sagebrush ecosystems.

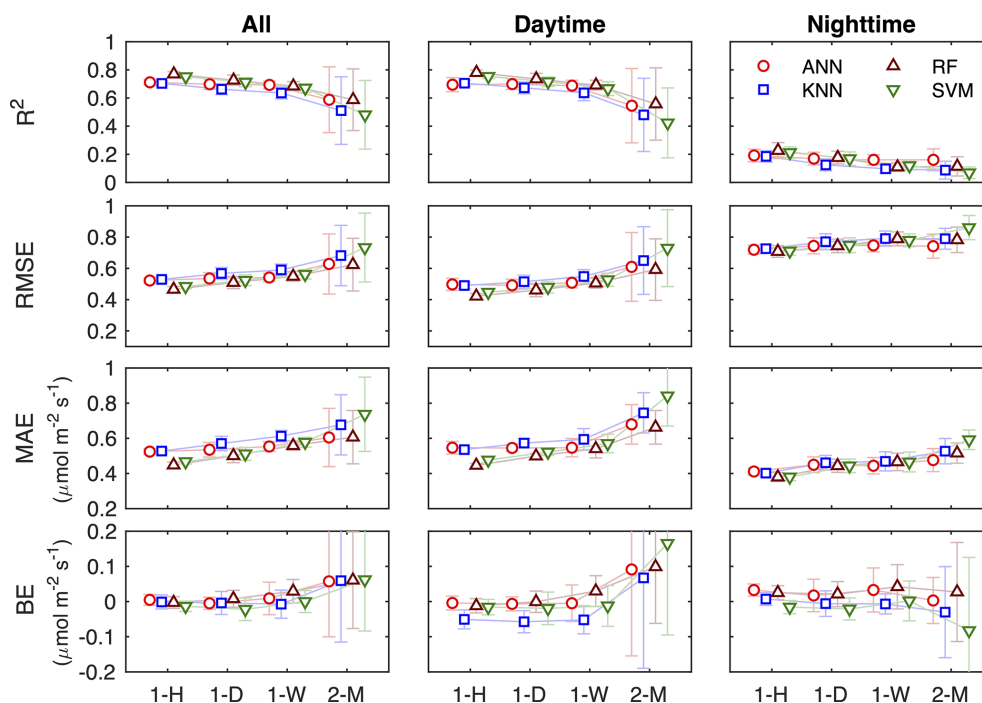
Following Moffat et al. (2007), we also perform the algorithm training and evaluation separately for daytime and nighttime data. For the daytime data, the performance of each algorithm is similar to that for all the data, whereas the algorithm performance for the nighttime data is degraded with R^2 of 0.1–0.2 and RMSE of 0.7–0.8, similar to the results for some forest sites in Moffat et al. (2007). The poor performance of the gap-filling algorithms for the nighttime data is primarily attributed to the shortage of available nighttime data for training the models (Fig. 2 and Table 1). However, the change of BE with the increased gap length at night is relatively small compared to that for the daytime data, especially for the ANN and RF. In addition, BE for long gaps (e.g., 2-M) has opposite signs for the daytime and nighttime data, resulting in a smaller BE for all the data.

3.3 Comparison of probability density functions (PDFs) between measured and estimated NEE

Figure 4 shows the comparison of the probability density functions (PDFs) between the measured and estimated NEE of the gap-filling algorithms. The estimated NEE by the gap-filling algorithms has a similar shape of PDFs, which is also quite similar to that of the measured NEE with some difference in amplitudes. At this site, the measured half-hourly NEE ranges from -6 to $4 \mu\text{mol m}^{-2} \text{s}^{-1}$, while the estimated NEE varies from approximately -5 to $2 \mu\text{mol m}^{-2} \text{s}^{-1}$. For all the data, the PDFs of the estimated NEE present two peaks at around -0.2 and $0.2 \mu\text{mol m}^{-2} \text{s}^{-1}$, whereas the PDF of the measured NEE only has one peak at around $0.2 \mu\text{mol m}^{-2} \text{s}^{-1}$. That means that the PDFs of the estimated NEE have a higher amplitude than the measured NEE in the range of -0.6 to $0.0 \mu\text{mol m}^{-2} \text{s}^{-1}$. However, in the range of -2.0 to $-0.8 \mu\text{mol m}^{-2} \text{s}^{-1}$, the amplitude of the PDFs of the estimated NEE is lower than that of the measured NEE. The PDFs of the estimated NEE for the daytime data show one peak at around $-0.2 \mu\text{mol m}^{-2} \text{s}^{-1}$, with their shapes similar to those for all the data in the range with the negative NEE values; for the nighttime data, the estimated NEE has a narrower shape of PDF than that of the measured NEE. These results suggest that the gap-filling algorithms underestimate the magnitudes of NEE in the range of -2.0 to $0.0 \mu\text{mol m}^{-2} \text{s}^{-1}$ and the magnitudes of the peak values of NEE.

Table 1. Percentage of NEE data with different gap scores (0/1/2) for daytime and nighttime from 2016 to 2019. NEE gaps are classified as non-gaps (gap score: 0), gaps due to low data quality (gap score: 1), and gaps due to electrical and/or instrument failures (gap score: 2).

	Daytime	Nighttime	All
2016	36.1%/9.6%/2.7%	19.9%/26.1%/5.6%	56.0%/35.7%/8.3%
2017	31.5%/9.8%/7.1%	15.4%/22.3%/13.9%	46.9%/32.1%/21.0%
2018	27.8%/6.8%/14.1%	10.9%/16.5%/23.9%	38.7%/23.3%/38.0%
2019	23.4%/7.1%/17.9%	10.0%/18.1%/23.5%	33.4%/25.2%/41.4%
Overall	29.7%/8.4%/10.5%	14.0%/20.7%/16.7%	43.7%/29.1%/27.2%

**Figure 3.** Performance of NEE gap-filling algorithms for the four gap length scenarios (i.e., 1 h (1-H), 1 d (1-D), 1 week (1-W), and 2 months (2-M)).

3.4 Comparison of measurement error and absolute error of ML algorithms

Figure 5 shows the absolute errors as a function of bin-averaged NEE values for the gap-filling algorithms with the estimated random measurement errors (Finkelstein and Sims, 2001) as a reference. For all the data, the binned absolute errors for the ML algorithms are quite close to each other, and they are also close to the random errors in the range of negative NEE values but slightly deviated from the random errors in the range of positive NEE values. Note that the large deviations from the random errors at the edges are most likely due to the small number of data points as illustrated in Fig. 4. The binned absolute errors for the daytime data are close to the random errors in the NEE range of about -4.0 to $1.0 \mu\text{mol m}^{-2} \text{s}^{-1}$, whereas the binned absolute errors for the nighttime data are consistently higher than the random errors. For all the data, the mean value of the

random errors is $0.56 \mu\text{mol m}^{-2} \text{s}^{-1}$, while the MAE of the ML algorithms is 0.55 , 0.59 , 0.53 , and $0.58 \mu\text{mol m}^{-2} \text{s}^{-1}$ for the ANN, KNN, RF, and SVM, respectively. For the daytime data, the MAE of the ML algorithms (0.59 , 0.62 , 0.55 , and $0.62 \mu\text{mol m}^{-2} \text{s}^{-1}$) is smaller than the mean value of the random error ($0.66 \mu\text{mol m}^{-2} \text{s}^{-1}$), whereas for the nighttime data, the MAE of the ML algorithms (0.46 , 0.48 , 0.47 , and $0.49 \mu\text{mol m}^{-2} \text{s}^{-1}$) is larger than the mean value of the random error ($0.32 \mu\text{mol m}^{-2} \text{s}^{-1}$). Overall, the RF and ANN have better performance in filling NEE gaps at this semi-arid site, especially for the daytime data, although the RF is more time efficient than the ANN. In addition, all four ML algorithms have low performance in gap-filling the nighttime data, though the BE for the nighttime data is relatively small compared to the daytime data mostly due to the low magnitudes of the nighttime NEE.

Table 2. Performance metrics of the four ML gap-filling algorithms for the four gap length scenarios. The ML algorithms are trained and evaluated without separating daytime and nighttime data.

Gap length scenarios		R^2	RMSE	MAE ($\mu\text{mol m}^{-2} \text{s}^{-1}$)	BE ($\mu\text{mol m}^{-2} \text{s}^{-1}$)
ANN	1 h	0.71 ± 0.02	0.52 ± 0.02	0.50 ± 0.01	-0.005 ± 0.016
	1 d	0.70 ± 0.02	0.54 ± 0.04	0.51 ± 0.02	0.005 ± 0.017
	1 week	0.69 ± 0.03	0.54 ± 0.03	0.51 ± 0.04	-0.009 ± 0.046
	2 months	0.59 ± 0.23	0.63 ± 0.19	0.62 ± 0.07	-0.057 ± 0.158
KNN	1 h	0.71 ± 0.02	0.53 ± 0.02	0.50 ± 0.01	0.001 ± 0.020
	1 d	0.66 ± 0.04	0.57 ± 0.04	0.55 ± 0.02	0.004 ± 0.033
	1 week	0.63 ± 0.05	0.59 ± 0.04	0.57 ± 0.06	0.007 ± 0.040
	2 months	0.51 ± 0.24	0.68 ± 0.19	0.69 ± 0.08	-0.059 ± 0.175
RF	1 h	0.77 ± 0.02	0.47 ± 0.02	0.43 ± 0.01	0.003 ± 0.017
	1 d	0.73 ± 0.04	0.51 ± 0.04	0.48 ± 0.02	-0.008 ± 0.024
	1 week	0.68 ± 0.03	0.55 ± 0.03	0.52 ± 0.05	-0.029 ± 0.033
	2 months	0.60 ± 0.22	0.62 ± 0.17	0.61 ± 0.05	-0.061 ± 0.137
SVM	1 h	0.75 ± 0.02	0.48 ± 0.02	0.45 ± 0.01	0.014 ± 0.015
	1 d	0.71 ± 0.03	0.52 ± 0.03	0.49 ± 0.02	0.022 ± 0.032
	1 week	0.67 ± 0.03	0.56 ± 0.03	0.53 ± 0.04	-0.000 ± 0.031
	2 months	0.47 ± 0.25	0.73 ± 0.22	0.77 ± 0.16	-0.062 ± 0.146

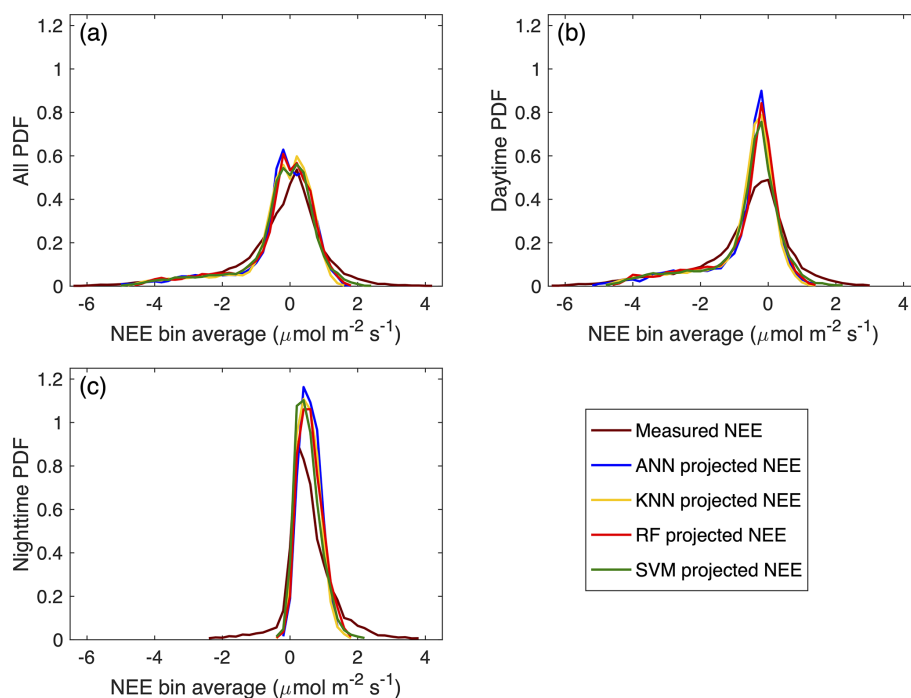


Figure 4. Comparison of probability density functions (PDFs) for the measured and estimated NEE of the gap-filling algorithms using daytime and nighttime data together and separately. The PDFs are estimated from the binned density distributions divided by the bin width. The bin width is $0.2 \mu\text{mol m}^{-2} \text{s}^{-1}$, and bins with fewer than 10 data points are excluded.

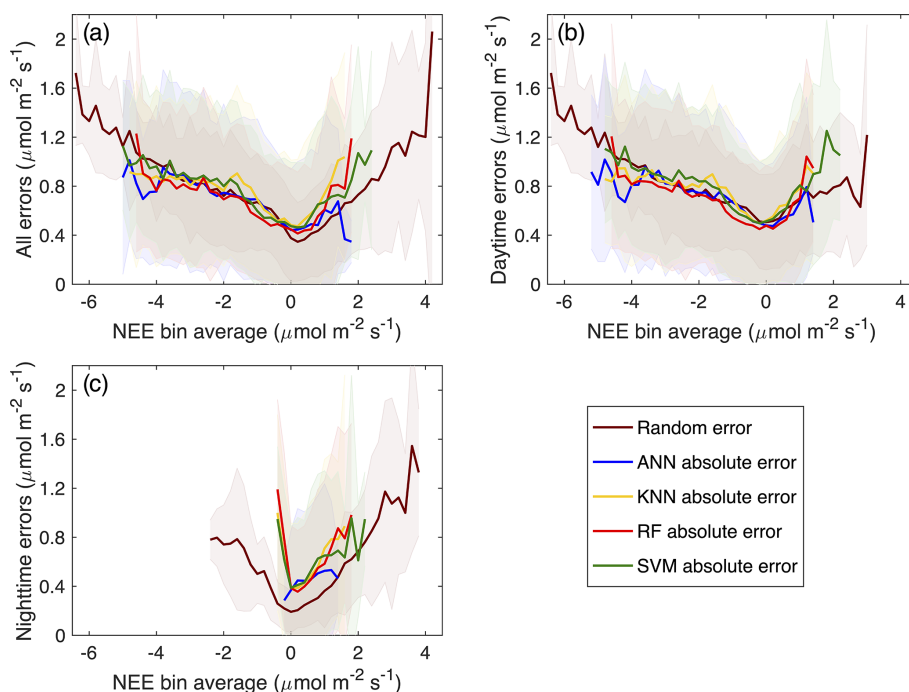


Figure 5. Comparison of NEE measurement and model uncertainties of the gap-filling algorithms using the data and the daytime and nighttime data. The random measurement error is estimated by Finkelstein and Sims (2001). The bin width is $0.2 \mu\text{mol m}^{-2} \text{s}^{-1}$, and bins with fewer than 10 data points are excluded.

4 Discussion

4.1 Uncertainties in carbon budgets caused by gap-filling

We now examine uncertainties in carbon budgets caused by gap filling with a different training dataset and different methods. Figure 6 compares the monthly NEE of the gap-filled data during 2016–2019. The subscript A denotes that the daytime and nighttime NEE data are gap-filled together using the ML algorithms trained with all the data, and DN denotes that the daytime and nighttime data are gap-filled separately using the trained ML algorithms and then combined together to determine the monthly NEE. The error bar denotes 1 standard deviation of the monthly NEE of the 40 gap-filled time series. Here the gap-filled NEE using the most commonly used MDS method is also included as a reference for comparison.

With the 40 gap-filled NEE time series for each method, we first investigate the self-agreement of each method as the method with good self-agreement should have small variations in the accumulative NEE among different trails. For months with gaps less than 7 d (Fig. 2; e.g., February to October in 2016), all four ML algorithms have good self-agreement, with the mean standard deviations of the monthly NEE ranging from 0.4 (ANN) to 1.0 (SVM) g C m^{-2} . Both the RF and KNN have mean standard deviations of approximately 0.7 g C m^{-2} during these months. For months with

long gaps (i.e., >7 d), the mean standard deviations of the monthly NEE are 1.2, 1.3, 1.5, and 3.3 g C m^{-2} for the ANN, KNN, RF, and SVM, respectively. From this perspective, the ANN is the most reliable method in gap-filling because the predicted values are averages of the 20 best runs (Sect. 2.4.1). In other words, most of the ML algorithms are quite consistent in filling the gaps, and the differences in the monthly NEE caused by changes in training dataset are less than 1.5 g C m^{-2} except for the SVM.

The uncertainties in the monthly NEE as a result of the differences in the methods are now assessed with the monthly NEE from the MDS as a reference. The difference among the methods ranges from 0.2 to 1.3 g C m^{-2} for months with gaps less than 7 d and ranges from 0.8 to 10.2 g C m^{-2} for months with long gaps, which is 0.8 to 4.8 g C m^{-2} without including the SVM. For the ANN and RF, the differences in the monthly NEE between A and DN are usually quite small for all the months, whereas the KNN presents opposite signs for A and DN in months with long gaps, which means that the KNN is unable to handle the daytime and nighttime data together. Overall, for months with short to medium gaps (i.e., <7 d), there is no significant difference in the monthly NEE among the methods including the MDS method. For months with long gaps (i.e., >7 d), the MDS method usually fails, and the ANN and RF have the best performance, and they have the potential to handle the daytime and nighttime data gap-filling together, as also supported by the distribution of estimated variable importance (Fig. 1).

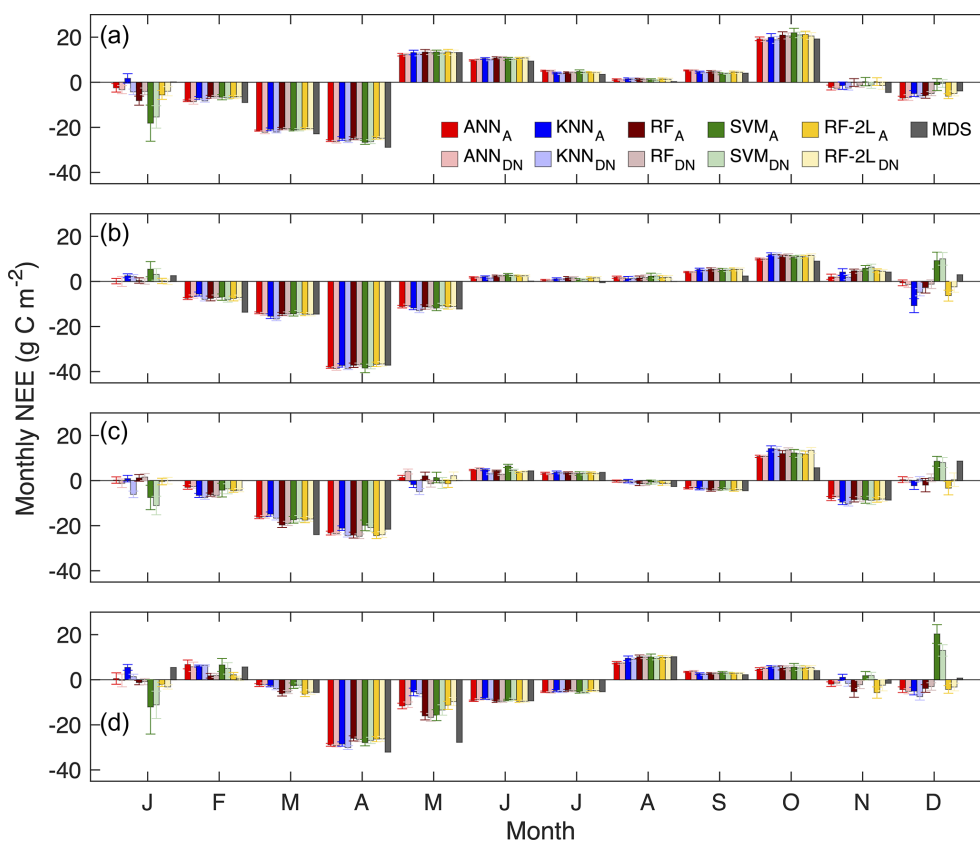


Figure 6. Monthly total net ecosystem exchange (NEE, g C m^{-2}) at the US-Hn1 in (a)–(d) 2016–2019. The subscript A denotes that the daytime and nighttime NEE data are gap-filled together using the ML algorithms trained with all the data, and DN denotes that the daytime and nighttime data are gap-filled separately and then combined to determine the monthly total values. RF-2L denotes the proposed two-layer RF-based gap-filling framework, and MDS is the marginal distribution sampling algorithm. The error bar denotes 1 standard deviation of the monthly total NEE of the 40 gap-filled time series.

The uncertainties in the annual total NEE are estimated by comparing the annual NEE obtained by each ML algorithm with their ensemble means (Fig. 7). Obviously, both the KNN and SVM are largely apart from the ensemble means, whereas the ANN and RF are relatively close to the ensemble means except for the RF in 2019. The mean standard deviations of the 40 trials for the annual NEE by ANN range from 2.5 to 4.3 g C m^{-2} , the mean standard deviations by the RF vary from 3.4 to 7.1 g C m^{-2} , and the mean standard deviations by the KNN and SVM vary from 5.1 to 13.9 g C m^{-2} . The differences between the ANN and RF are within $\pm 8.4 \text{ g C m}^{-2}$, and the differences between A and DN are less than 1.7 and 4.5 g C m^{-2} for the ANN and RF, respectively. The overall uncertainties in the annual NEE caused by the ANN and RF are usually less than 15.5 g C m^{-2} , while the uncertainties can be as large as 27.2 g C m^{-2} if including the KNN and SVM. Therefore, it is recommended to use the ensemble mean of the ANN and RF as the best estimate of the annual NEE at the semiarid sagebrush site. The annual mean NEE by the ANN and RF is -15.4 ± 4.7 , -50.0 ± 9.1 , -31.4 ± 7.2 , and

$-40.3 \pm 8.7 \text{ g C m}^{-2}$ for 2016, 2017, 2018, and 2019, respectively. In addition, the annual total NEE by the MDS is about 5.6–15.6 g C m^{-2} larger than that by the ANN and RF.

4.2 Performance of the two-layer RF-based gap-filling framework (RF-2L)

Following the same procedures as for evaluating the ML algorithms above, the performance of RF-2L in filling the long gaps (i.e., 2 months) in the daytime and nighttime daily means is also accessed. Using a 10-fold cross-validation repeated 10 times, the R^2 of the second-layer RF model is 0.78, 0.85, and 0.77 for all the data, the daytime data, and the nighttime data, respectively. The mean BE for this framework is $0.04 \text{ g C m}^{-2} \text{ d}^{-1}$, which is slightly smaller than that of the original RF with the half-hourly NEE data ($0.06 \text{ g C m}^{-2} \text{ d}^{-1}$).

The uncertainties of the RF-2L are accessed by comparing the monthly and annual NEE with other ML algorithms. As shown in Figs. 6 and 7, the monthly and annual NEEs by the RF-2L are quite close to those by the RF. For A (i.e., trained by all the data), the difference in the annual mean

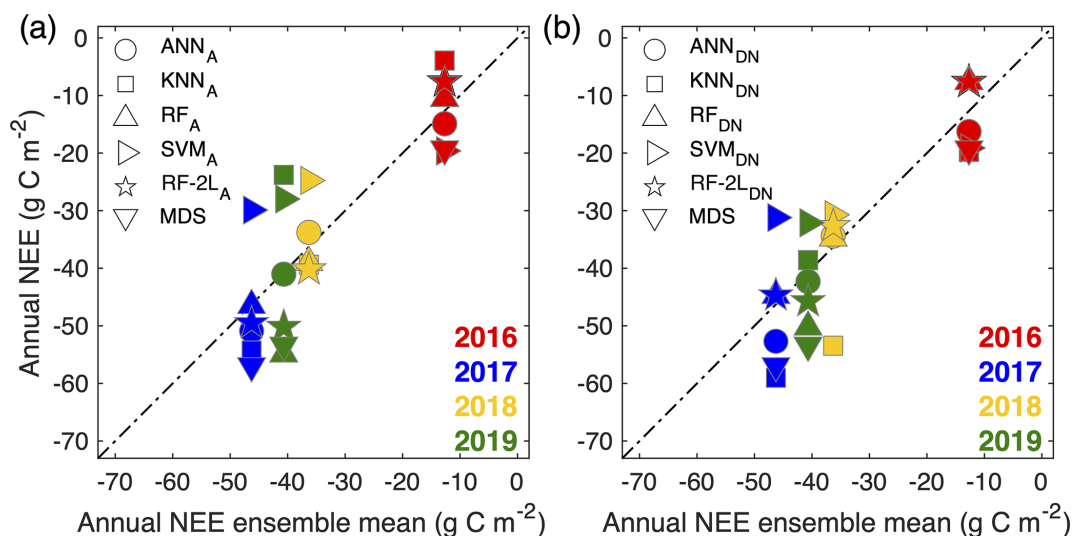


Figure 7. Comparison of the annual mean NEE from the ML algorithms and their ensemble mean. The subscript A denotes that daytime and nighttime NEE data are gap-filled together using the ML algorithms trained with all the data, and DN denotes that the daytime and nighttime data are gap-filled separately and then combined to determine the monthly total values.

NEE ranges from 0.0 to 2.2 g C m⁻², whereas for DN (i.e., trained by the separated daytime and nighttime data), the difference varies from 0.8 to 3.3 g C m⁻². This test suggests that it is not necessary to fill all the gaps in the half-hourly NEE data if the focus is on assessing the uncertainties in annual mean NEE and interannual variability. Therefore, the RF-2L provides an alternative in filling extremely long gaps to characterize annual carbon budgets and interannual variability in dryland ecosystems. In addition, the performance of the different ML algorithms is quite consistent when filling short to medium gaps (e.g., <7 d), and thus a promising extension of the proposed approach is that using the ensemble mean of multiple methods as the input of the second RF layer, which may have the potential to lower the uncertainties in the gap-filled data. Of course, other reliable algorithms can also be applied in the second layer to reduce bias estimation caused by long gaps.

5 Conclusions

The performance of the four ML algorithms in filling the NEE data gaps is evaluated at a semiarid sagebrush ecosystem site. Due to the relatively small range of NEE variations, the overall performance of these gap-filling algorithms at this site is lower than that at other forest sites but comparable to that at other grassland sites. The RF algorithm outperforms the other algorithms in terms of the overall performance. It is not necessary to train the model separately for daytime and nighttime data when using the ANN and RF algorithms. The uncertainties in the monthly and annual NEEs due to the gap-filling approaches are evaluated by the standard deviations of monthly NEE of multiple trials for each method and also

accessed by the difference in the monthly NEE by the methods. With the ANN and RF, the uncertainties in annual NEE are usually within 16 g C m⁻² at this semiarid sagebrush site. Extremely long gaps in half-hourly NEE data due to power failures cannot be confidently filled by either of the methods because of the high uncertainties in R^2 and RMSE, and thus we propose and test a two-layer RF-based gap-filling framework. With this framework, the improvement in model performance is significant, especially for the nighttime data. Therefore, it is recommended that the two-layer RF-based framework (RF-2L) be used if there are extremely long gaps existed in the NEE dataset and if there is a need to investigate its annual and interannual variability. However, it is hard to assess the uncertainties caused by bias in the gap-filled meteorological variables using the current approaches and study design, which need to be explored in future studies.

Code availability. The code used in this study is available from Jingyu Yao and Jianping Huang upon request.

Data availability. The data used in this study are deposited in a public domain repository at <https://doi.org/10.6084/m9.figshare.14747952> (Yao et al., 2021).

Author contributions. JY, ZG, and HL contributed equally to this work. JH designed the study with substantial input from all coauthors. ZG and HL conducted the fieldwork and obtained and processed the EC data. JY performed the gap-filling and analyzed the results. JY and ZG drafted the manuscript. JH, HL, and GW con-

tributed to the result analysis and interpretation. All authors commented on and approved the final paper.

Competing interests. Some authors are members of the editorial board of *Atmospheric Chemistry and Physics*. The peer-review process was guided by an independent editor, and the authors have also no other competing interests to declare.

Disclaimer. Publisher's note: Copernicus Publications remains neutral with regard to jurisdictional claims in published maps and institutional affiliations.

Acknowledgements. We thank Justine Missik, Eric Russell, Evan Arntzen, Douglas McFarland, Brittany Verbeke, Xingyuan Chen, Maoyi Huang, and many other participants for their assistance in the field. We thank the researchers and contributors of the MODIS products and AWN weather data.

Financial support. This research has been supported by the Second Tibetan Plateau Scientific Expedition and Research Program (STEP) (grant no. 2019QZKK0602), the National Natural Science Foundation of China (grant nos. 41521004, 41991231, and 41975075), the Foundation of Key Laboratory for Semi-Arid Climate Change of the Ministry of Education in Lanzhou University, the China 111 Project (grant no. B13045), the U.S. National Science Foundation (grant nos. NSF-AGS-1419614 and NSF-AGS-1853050), and the U.S. Department of Energy (DOE) Office of Biological and Environmental Research (BER) as part of BER's Subsurface Biogeochemistry Research Program (SBR) at the Pacific Northwest National Laboratory (PNNL). PNNL is operated by Battelle Memorial Institute for the U.S. DOE (grant no. DE-AC05-76RL01830).

Review statement. This paper was edited by Hailong Wang and reviewed by two anonymous referees.

References

- Ahlström, A., Raupach, M. R., Schurgers, G., Smith, B., Arneth, A., Jung, M., Reichstein, M., Canadell, J. G., Friedlingstein, P., Jain, A. K., Kato, E., Poulter, B., Sitch, S., Stocker, B. D., Viivy, N., Wang, Y. P., Wiltshire, A., Zaehle, S., and Zeng, N.: The dominant role of semi-arid ecosystems in the trend and variability of the land CO₂ sink, *Science*, 348, 895–899, <https://doi.org/10.1126/science.aaa1668>, 2015.
- Aubinet, M., Vesala, T., and Papale, D. (Eds.): *Eddy Covariance: A Practical Guide to Measurement and Data Analysis*, Springer, Dordrecht, the Netherlands, 438 pp., <https://doi.org/10.1007/978-94-007-2351-1>, 2012.
- Baldocchi, D. and Sturtevant, C.: Does day and night sampling reduce spurious correlation between canopy photosynthesis and ecosystem respiration?, *Agr. Forest Meteorol.*, 207, 117–126, <https://doi.org/10.1016/j.agrformet.2015.03.010>, 2015.
- Baldocchi, D. D.: Assessing the eddy covariance technique for evaluating carbon dioxide exchange rates of ecosystems: past, present and future, *Glob. Change Biol.*, 9, 479–492, <https://doi.org/10.1046/j.1365-2486.2003.00629.x>, 2003.
- Berg, A. and McColl, K. A.: No projected global drylands expansion under greenhouse warming, *Nat. Clim. Chang.*, 11, 331–337, <https://doi.org/10.1038/s41558-021-01007-8>, 2021.
- Biederman, J. A., Scott, R. L., Bell, T. W., Bowling, D. R., Dore, S., Garatuza-Payan, J., Kolb, T. E., Krishnan, P., Krofcheck, D. J., Litvak, M. E., Maurer, G. E., Meyers, T. P., OECHEL, W. C., Papuga, S. A., Ponce-Campos, G. E., Rodriguez, J. C., Smith, W. K., Vargas, R., Watts, C. J., Yezpe, E. A., Goulden, M. L., Garatuza Payan, J., Kolb, T. E., Krishnan, P., Krofcheck, D. J., Litvak, M. E., Maurer, G. E., Meyers, T. P., OECHEL, W. C., Papuga, S. A., Ponce-Campos, G. E., Rodriguez, J. C., Smith, W. K., Vargas, R., Watts, C. J., Yezpe, E. A., and Goulden, M. L.: CO₂ exchange and evapotranspiration across dryland ecosystems of southwestern North America, *Glob. Change Biol.*, 23, 4204–4221, <https://doi.org/10.1111/gcb.13686>, 2017.
- Breiman, L.: Random forests, *Mach. Learn.*, 45, 5–32, <https://doi.org/10.1023/A:1010933404324>, 2001.
- Chen, Y. Y., Chu, C. R., and Li, M. H.: A gap-filling model for eddy covariance latent heat flux: Estimating evapotranspiration of a subtropical seasonal evergreen broad-leaved forest as an example, *J. Hydrol.*, 468–469, 101–110, <https://doi.org/10.1016/j.jhydrol.2012.08.026>, 2012.
- Chu, H., Luo, X., Ouyang, Z., Chan, W. S., Dengel, S., Biraud, S. C., Torn, M. S., Metzger, S., Kumar, J., Arain, M. A., Arkebauer, T. J., Baldocchi, D., Bernacchi, C., Billesbach, D., Black, T. A., Blanken, P. D., Bohrer, G., Bracho, R., Brown, S., Brunzell, N. A., Chen, J., Chen, X., Clark, K., Desai, A. R., Duman, T., Durden, D., Fares, S., Forbrich, I., Gamon, J. A., Gough, C. M., Griffis, T., Helbig, M., Hollinger, D., Humphreys, E., Ikawa, H., Iwata, H., Ju, Y., Knowles, J. F., Knox, S. H., Kobayashi, H., Kolb, T., Law, B., Lee, X., Litvak, M., Liu, H., Munger, J. W., Noormets, A., Novick, K., Oberbauer, S. F., Oechel, W., Oikawa, P., Papuga, S. A., Pendall, E., Prajapati, P., Prueger, J., Quinton, W. L., Richardson, A. D., Russell, E. S., Scott, R. L., Starr, G., Staebler, R., Stoy, P. C., Stuart-Haëntjens, E., Sonnentag, O., Sullivan, R. C., Suyker, A., Ueyama, M., Vargas, R., Wood, J. D., and Zona, D.: Representativeness of Eddy-Covariance flux footprints for areas surrounding AmeriFlux sites, *Agr. Forest Meteorol.*, 301–302, 108350, <https://doi.org/10.1016/J.AGRFORMET.2021.108350>, 2021.
- Cortes, C. and Vapnik, V.: Support-vector networks, *Mach. Learn.*, 20, 273–297, <https://doi.org/10.1007/bf00994018>, 1995.
- Delwiche, K. B., Knox, S. H., Malhotra, A., Fluet-Chouinard, E., McNicol, G., Feron, S., Ouyang, Z., Papale, D., Trotta, C., Canfora, E., Cheah, Y.-W., Christianson, D., Alberto, Ma. C. R., Alekseychik, P., Aurela, M., Baldocchi, D., Bansal, S., Billesbach, D. P., Bohrer, G., Bracho, R., Buchmann, N., Campbell, D. I., Celis, G., Chen, J., Chen, W., Chu, H., Dalmagro, H. J., Dengel, S., Desai, A. R., Detto, M., Dolman, H., Eichelmann, E., Euskirchen, E., Famulari, D., Fuchs, K., Goeckede, M., Gogo, S., Gondwe, M. J., Goodrich, J. P., Gottschalk, P., Graham, S. L., Heimann, M., Helbig, M., Helfter, C., Hemes, K. S., Hirano, T., Hollinger, D., Hörtnagl, L., Iwata, H., Jacotot, A., Jurasinski, G.,

- Kang, M., Kasak, K., King, J., Klatt, J., Koebisch, F., Krauss, K. W., Lai, D. Y. F., Lohila, A., Mammarella, I., Belelli Marchesini, L., Manca, G., Matthes, J. H., Maximov, T., Merbold, L., Mitra, B., Morin, T. H., Nemitz, E., Nilsson, M. B., Niu, S., Oechel, W. C., Oikawa, P. Y., Ono, K., Peichl, M., Peltola, O., Reba, M. L., Richardson, A. D., Riley, W., Runkle, B. R. K., Ryu, Y., Sachs, T., Sakabe, A., Sanchez, C. R., Schuur, E. A., Schäfer, K. V. R., Sonntag, O., Sparks, J. P., Stuart-Haëntjens, E., Sturtevant, C., Sullivan, R. C., Szutu, D. J., Thom, J. E., Torn, M. S., Tuittila, E.-S., Turner, J., Ueyama, M., Valach, A. C., Vargas, R., Varlagin, A., Vazquez-Lule, A., Verfaillie, J. G., Vesala, T., Vourlitis, G. L., Ward, E. J., Wille, C., Wohlfahrt, G., Wong, G. X., Zhang, Z., Zona, D., Windham-Myers, L., Poulter, B., and Jackson, R. B.: FLUXNET-CH₄: a global, multi-ecosystem dataset and analysis of methane seasonality from freshwater wetlands, *Earth Syst. Sci. Data*, 13, 3607–3689, <https://doi.org/10.5194/essd-13-3607-2021>, 2021.
- Dengel, S., Zona, D., Sachs, T., Aurela, M., Jammert, M., Parmentier, F. J. W., Oechel, W., and Vesala, T.: Testing the applicability of neural networks as a gap-filling method using CH₄ flux data from high latitude wetlands, *Biogeosciences*, 10, 8185–8200, <https://doi.org/10.5194/bg-10-8185-2013>, 2013.
- Didan, K.: MOD13Q1 MODIS/Terra Vegetation Indices 16-Day L3 Glob. 250m SIN Grid V006, NASA EOSDI [data set], <https://doi.org/10.5067/MODIS/MOD13Q1.006>, 2015.
- Dragoni, D., Schmid, H. P., Grimmond, C. S. B., and Loescher, H. W.: Uncertainty of annual net ecosystem productivity estimated using eddy covariance flux measurements, *J. Geophys. Res.-Atmos.*, 112, 17102, <https://doi.org/10.1029/2006JD008149>, 2007.
- Falge, E., Baldocchi, D., Olson, R., Anthoni, P., Aubinet, M., Bernhofer, C., Burba, G., Ceulemans, R., Clement, R., Dolman, H., Granier, A., Gross, P., Grünwald, T., Hollinger, D., Jensen, N. O., Katul, G., Keronen, P., Kowalski, A., Lai, C. T., Law, B. E., Meyers, T., Moncrieff, J., Moors, E., Munger, J. W., Pilegaard, K., Rannik, Ü., Rebmann, C., Suyker, A., Tenhunen, J., Tu, K., Verma, S., Vesala, T., Wilson, K., and Wofsy, S.: Gap filling strategies for defensible annual sums of net ecosystem exchange, *Agr. Forest Meteorol.*, 107, 43–69, [https://doi.org/10.1016/S0168-1923\(00\)00225-2](https://doi.org/10.1016/S0168-1923(00)00225-2), 2001.
- Feng, S. and Fu, Q.: Expansion of global drylands under a warming climate, *Atmos. Chem. Phys.*, 13, 10081–10094, <https://doi.org/10.5194/acp-13-10081-2013>, 2013.
- Finkelstein, P. L. and Sims, P. F.: Sampling error in eddy correlation flux measurements, *J. Geophys. Res.-Atmos.*, 106, 3503–3509, <https://doi.org/10.1029/2000JD900731>, 2001.
- Fix, E. and Hodges, J. L.: Discriminatory analysis. Nonparametric discrimination; consistency properties, Report Number 4, Project Number 21-49-004, USAF School of Aviation Medicine, Randolph Field, Texas, 1951.
- Gao, Z., Russell, E. S., Missik, J. E. C., Huang, M., Chen, X., Strickland, C. E., Clayton, R., Arntzen, E., Ma, Y., and Liu, H.: A novel approach to evaluate soil heat flux calculation: An analytical review of nine methods, *J. Geophys. Res.*, 122, 6934–6949, <https://doi.org/10.1002/2017JD027160>, 2017.
- Gao, Z., Liu, H., Missik, J. E. C., Yao, J., Huang, M., Chen, X., Arntzen, E., and McFarland, D. P.: Mechanistic links between underestimated CO₂ fluxes and non-closure of the surface energy balance in a semi-arid sagebrush ecosystem, *Environ. Res. Lett.*, 14, 044016, <https://doi.org/10.1088/1748-9326/ab082d>, 2019.
- Gao, Z., Liu, H., Chen, X., Huang, M., Missik, J. E. C., Yao, J., Arntzen, E., and McFarland, D. P.: Enlarged non-closure of surface energy balance with increasing atmospheric instabilities linked to changes in coherent structures, *J. Geophys. Res.-Atmos.*, 125, e2020JD032889, <https://doi.org/10.1029/2020jd032889>, 2020a.
- Gao, Z., Liu, H., Arntzen, E., McFarland, D. P., Chen, X., and Huang, M.: Uncertainties in Turbulent Statistics and Fluxes of CO₂ Associated With Density Effect Corrections, *Geophys. Res. Lett.*, 47, e2020GL088859, <https://doi.org/10.1029/2020GL088859>, 2020b.
- Günther, F. and Fritsch, S.: Neuralnet: Training of neural networks, *R Journal*, 2, 30–38, <https://doi.org/10.32614/rj-2010-006>, 2010.
- Huang, I.-H. and Hsieh, C.-I.: Gap-Filling of Surface Fluxes Using Machine Learning Algorithms in Various Ecosystems, *Water*, 12, 3415, <https://doi.org/10.3390/w12123415>, 2020.
- Huang, J., Yu, H., Guan, X., Wang, G., and Guo, R.: Accelerated dryland expansion under climate change, *Nat. Clim. Chang.*, 6, 166–171, <https://doi.org/10.1038/nclimate2837>, 2016.
- Irvin, J., Zhou, S., McNicol, G., Lu, F., Liu, V., Fluet-Chouinard, E., Ouyang, Z., Knox, S. H., Lucas-Moffat, A., Trotta, C., Papale, D., Vitale, D., Mammarella, I., Alekseychik, P., Aurela, M., Avati, A., Baldocchi, D., Bansal, S., Bohrer, G., Campbell, D. I., Chen, J., Chu, H., Dalmagro, H. J., Delwiche, K. B., Desai, A. R., Euskirchen, E., Feron, S., Goeckede, M., Heimann, M., Helbig, M., Helfter, C., Hemes, K. S., Hirano, T., Iwata, H., Jurasinski, G., Kalhori, A., Kondrich, A., Lai, D. Y., Lohila, A., Malhotra, A., Merbold, L., Mitra, B., Ng, A., Nilsson, M. B., Noormets, A., Peichl, M., Rey-Sanchez, A. C., Richardson, A. D., Runkle, B. R., Schäfer, K. V., Sonntag, O., Stuart-Haëntjens, E., Sturtevant, C., Ueyama, M., Valach, A. C., Vargas, R., Vourlitis, G. L., Ward, E. J., Wong, G. X., Zona, D., Alberto, M. C. R., Billesbach, D. P., Celis, G., Dolman, H., Friborg, T., Fuchs, K., Gogo, S., Gondwe, M. J., Goodrich, J. P., Gottschalk, P., Hörtnagl, L., Jacotot, A., Koebisch, F., Kasak, K., Maier, R., Morin, T. H., Nemitz, E., Oechel, W. C., Oikawa, P. Y., Ono, K., Sachs, T., Sakabe, A., Schuur, E. A., Shortt, R., Sullivan, R. C., Szutu, D. J., Tuittila, E. S., Varlagin, A., Verfaillie, J. G., Wille, C., Windham-Myers, L., Poulter, B., and Jackson, R. B.: Gap-filling eddy covariance methane fluxes: Comparison of machine learning model predictions and uncertainties at FLUXNET-CH₄ wetlands, *Agr. Forest Meteorol.*, 308–309, 108528, <https://doi.org/10.1016/J.AGRFORMET.2021.108528>, 2021.
- Jammert, M., Crill, P., Dengel, S., and Friborg, T.: Large methane emissions from a subarctic lake during spring thaw: Mechanisms and landscape significance, *J. Geophys. Res.-Biogeo.*, 120, 2289–2305, <https://doi.org/10.1002/2015JG003137>, 2015.
- Jung, M., Reichstein, M., Schwalm, C. R., Huntingford, C., Sitch, S., Ahlström, A., Arneth, A., Camps-Valls, G., Ciais, P., Friedlingstein, P., Gans, F., Ichii, K., Jain, A. K., Kato, E., Papale, D., Poulter, B., Raduly, B., Rödenbeck, C., Tramontana, G., Viovy, N., Wang, Y. P., Weber, U., Zaehle, S., and Zeng, N.: Compensatory water effects link yearly global land CO₂ sink changes to temperature, *Nature*, 541, 516–520, <https://doi.org/10.1038/nature20780>, 2017.

- Karatzoglou, A., Smola, A., Hornik, K., and Zeileis, A.: kernlab – An S4 Package for Kernel Methods in R, *J. Stat. Softw.*, 11, 1–20, <https://doi.org/10.18637/jss.v011.i09>, 2004.
- Kim, Y., Johnson, M. S., Knox, S. H., Black, T. A., Dalmagro, H. J., Kang, M., Kim, J., and Baldocchi, D.: Gap-filling approaches for eddy covariance methane fluxes: A comparison of three machine learning algorithms and a traditional method with principal component analysis, *Glob. Chang. Biol.*, 26, 1499–1518, <https://doi.org/10.1111/gcb.14845>, 2020.
- Knox, S. H., Matthes, J. H., Sturtevant, C., Oikawa, P. Y., Verfaillie, J., and Baldocchi, D.: Biophysical controls on interannual variability in ecosystem-scale CO₂ and CH₄ exchange in a California rice paddy, *J. Geophys. Res.-Biogeo.*, 121, 978–1001, <https://doi.org/10.1002/2015JG003247>, 2016.
- Kuhn, M., Wing, J., Weston, S., Williams, A., Keefer, C., Engelhardt, A., Cooper, T., Mayer, Z., Kenkel, B., Team, R. C., Benesty, M., Lescarbeau, R., Ziem, A., Scrucca, L., Tang, Y., Candan, C., and Hunt, T.: caret: Classification and Regression Training, cran [code], available at: <https://cran.r-project.org/package=caret>, last access: 15 April 2020.
- Liaw, A. and Wiener, M.: Classification and Regression by random Forest, *R News*, 2, 18–22, 2002.
- Mahabbati, A., Beringer, J., Leopold, M., McHugh, I., Cleverly, J., Isaac, P., and Izady, A.: A comparison of gap-filling algorithms for eddy covariance fluxes and their drivers, *Geosci. Instrum. Method. Data Syst.*, 10, 123–140, <https://doi.org/10.5194/gi-10-123-2021>, 2021.
- Ma, S., Baldocchi, D. D., Xu, L., and Hehn, T.: Inter-annual variability in carbon dioxide exchange of an oak/grass savanna and open grassland in California, *Agr. Forest Meteorol.*, 147, 157–171, <https://doi.org/10.1016/j.agrformet.2007.07.008>, 2007.
- Massman, W. J.: A simple method for estimating frequency response corrections for eddy covariance systems, *Agr. Forest Meteorol.*, 104, 185–198, [https://doi.org/10.1016/S0168-1923\(00\)00164-7](https://doi.org/10.1016/S0168-1923(00)00164-7), 2000.
- Massman, W. J.: Reply to comment by Rannik on “A simple method for estimating frequency response corrections for eddy covariance systems, *Agr. Forest Meteorol.*, 107, 247–251, [https://doi.org/10.1016/S0168-1923\(00\)00237-9](https://doi.org/10.1016/S0168-1923(00)00237-9), 2001.
- Mauder, M. and Foken, T.: Documentation and Instruction Manual of the Eddy Covariance Software Package TK2, 2004.
- Metzger, S.: Surface-atmosphere exchange in a box: Making the control volume a suitable representation for in-situ observations, *Agr. Forest Meteorol.*, 255, 68–80, <https://doi.org/10.1016/J.AGRFORMET.2017.08.037>, 2018.
- Missik, J. E. C., Liu, H., Gao, Z., Huang, M., Chen, X., Arntzen, E., McFarland, D. P., Ren, H., Titzler, P. S., Thomle, J. N., and Goldman, A.: Groundwater-River Water Exchange Enhances Growing Season Evapotranspiration and Carbon Uptake in a Semi-arid Riparian Ecosystem, *J. Geophys. Res.-Biogeo.*, 124, 99–114, <https://doi.org/10.1029/2018JG004666>, 2019.
- Missik, J. E. C., Liu, H., Gao, Z., Huang, M., Chen, X., Arntzen, E., McFarland, D. P., and Verbeke, B.: Groundwater Regulates Interannual Variations in Evapotranspiration in a Riparian Semi-arid Ecosystem, *J. Geophys. Res.-Atmos.*, 126, e2020JD033078, <https://doi.org/10.1029/2020jd033078>, 2021.
- Moffat, A. M., Papale, D., Reichstein, M., Hollinger, D. Y., Richardson, A. D., Barr, A. G., Beckstein, C., Braswell, B. H., Churkina, G., Desai, A. R., Falge, E., Gove, J. H., Heimann, M., Hui, D., Jarvis, A. J., Kattge, J., Noormets, A., and Stauch, V. J.: Comprehensive comparison of gap-filling techniques for eddy covariance net carbon fluxes, *Agr. Forest Meteorol.*, 147, 209–232, <https://doi.org/10.1016/j.agrformet.2007.08.011>, 2007.
- Moncrieff, J., Clement, R., Finnigan, J., and Meyers, T.: Averaging, Detrending, and Filtering of Eddy Covariance Time Series, in: *Handbook of Micrometeorology*, edited by: Lee, X., Massman, W., and Law, B., Springer, Dordrecht, 7–31 pp., <https://doi.org/10.1007/1-4020-2265-4>, 2004.
- Oncley, S., Foken, T., Vogt, R., Kohsiek, W., DeBruin, H. A. R., Bernhofer, C., Christen, A., Gorsel, E., Grantz, D., Feigenwinter, C., Lehner, I., Liebethal, C., Liu, H., Mauder, M., Pitacco, A., Ribeiro, L., and Weidinger, T.: The Energy Balance Experiment EBEX-2000. Part I: overview and energy balance, *Bound.-Lay. Meteorol.*, 123, 1–28, <https://doi.org/10.1007/s10546-007-9161-1>, 2007.
- Papale, D. and Valentini, R.: A new assessment of European forests carbon exchanges by eddy fluxes and artificial neural network spatialization, *Glob. Chang. Biol.*, 9, 525–535, <https://doi.org/10.1046/j.1365-2486.2003.00609.x>, 2003.
- Pastorello, G., Trotta, C., Canfora, E. et al.: The FLUXNET2015 dataset and the ONEFlux processing pipeline for eddy covariance data, *Sci. data*, 7, 225, <https://doi.org/10.1038/s41597-020-0534-3>, 2020.
- Reichstein, M., Falge, E., Baldocchi, D., Papale, D., Aubinet, M., Berbigier, P., Bernhofer, C., Buchmann, N., Gilmanov, T., Granier, A., Grünwald, T., Havránková, K., Ilvesniemi, H., Janous, D., Knohl, A., Laurila, T., Lohila, A., Loustau, D., Mat-teucci, G., Meyers, T., Miglietta, F., Ourcival, J. M., Pumpanen, J., Rambal, S., Rotenberg, E., Sanz, M., Tenhunen, J., Seufert, G., Vaccari, F., Vesala, T., Yakir, D., and Valentini, R.: On the separation of net ecosystem exchange into assimilation and ecosystem respiration: Review and improved algorithm, *Glob. Chang. Biol.*, 11, 1424–1439, <https://doi.org/10.1111/j.1365-2486.2005.001002.x>, 2005.
- Richardson, A. D. and Hollinger, D. Y.: A method to estimate the additional uncertainty in gap-filled NEE resulting from long gaps in the CO₂ flux record, *Agr. Forest Meteorol.*, 147, 199–208, <https://doi.org/10.1016/j.agrformet.2007.06.004>, 2007.
- Richardson, A. D., Mahecha, M. D., Falge, E., Kattge, J., Mof-fat, A. M., Papale, D., Reichstein, M., Stauch, V. J., Braswell, B. H., Churkina, G., Kruijt, B., and Hollinger, D. Y.: Statistical properties of random CO₂ flux measurement uncertainty inferred from model residuals, *Agr. Forest Meteorol.*, 148, 38–50, <https://doi.org/10.1016/J.AGRFORMET.2007.09.001>, 2008.
- Scott, R. L., Biederman, J. A., Hamerlynck, E. P., Barron Gafford, G. A., and Barron-Gafford, G. A.: The carbon balance pivot point of southwestern U.S. semiarid ecosystems: Insights from the 21st century drought, *J. Geophys. Res.-Biogeo.*, 120, 2612–2624, <https://doi.org/10.1002/2015JG003181>, 2015.
- Soloway, A. D., Amiro, B. D., Dunn, A. L., and Wofsy, S. C.: Carbon neutral or a sink? Uncertainty caused by gap-filling long-term flux measurements for an old-growth boreal black spruce forest, *Agr. Forest Meteorol.*, 233, 110–121, <https://doi.org/10.1016/j.agrformet.2016.11.005>, 2017.
- Stoy, P. C., Mauder, M., Foken, T., Marcolla, B., Boegh, E., Ibrom, A., Arain, M. A., Arneth, A., Aurela, M., Bernhofer, C., Cescatti, A., Dellwik, E., Duce, P., Gianelle, D., van Gorsel, E., Kiely, G., Knohl, A., Margolis, H., McCaughey, H., Mer-

- bold, L., Montagnani, L., Papale, D., Reichstein, M., Saunders, M., Serrano-Ortiz, P., Sottocornola, M., Spano, D., Vaccari, F., and Varlagin, A.: A data-driven analysis of energy balance closure across FLUXNET research sites: The role of landscape scale heterogeneity, *Agr. Forest Meteorol.*, 171–172, 137–152, <https://doi.org/10.1016/j.agrformet.2012.11.004>, 2013.
- Tramontana, G., Jung, M., Schwalm, C. R., Ichii, K., Camps-Valls, G., Ráduly, B., Reichstein, M., Arain, M. A., Cescatti, A., Kiely, G., Merbold, L., Serrano-Ortiz, P., Sickert, S., Wolf, S., and Papale, D.: Predicting carbon dioxide and energy fluxes across global FLUXNET sites with regression algorithms, *Biogeosciences*, 13, 4291–4313, <https://doi.org/10.5194/bg-13-4291-2016>, 2016.
- Webb, E. K., Pearman, G. I., and Leuning, R.: Correction of flux measurements for density effects due to heat and water vapour transfer, *Q. J. Roy. Meteorol. Soc.*, 106, 85–100, <https://doi.org/10.1002/qj.49710644707>, 1980.
- Wilson, K., Goldstein, A., Falge, E., Aubinet, M., Baldocchi, D., Berbigier, P., Bernhofer, C., Ceulemans, R., Dolman, H., Field, C., Grelle, A., Ibrom, A., Law, B. E., Kowalski, A., Meyers, T., Moncrieff, J., Monson, R., Oechel, W., Tenhunen, J., Valentini, R., and Verma, S.: Energy balance closure at FLUXNET sites, *Agr. Forest Meteorol.*, 113, 223–243, [https://doi.org/10.1016/S0168-1923\(02\)00109-0](https://doi.org/10.1016/S0168-1923(02)00109-0), 2002.
- Wutzler, T., Lucas-Moffat, A., Migliavacca, M., Knauer, J., Sickel, K., Šigut, L., Menzer, O., and Reichstein, M.: Basic and extensible post-processing of eddy covariance flux data with REddyProc, *Biogeosciences*, 15, 5015–5030, <https://doi.org/10.5194/bg-15-5015-2018>, 2018.
- Xu, T., Guo, Z., Liu, S., He, X., Meng, Y., Xu, Z., Xia, Y., Xiao, J., Zhang, Y., Ma, Y., and Song, L.: Evaluating Different Machine Learning Methods for Upscaling Evapotranspiration from Flux Towers to the Regional Scale, *J. Geophys. Res.-Atmos.*, 123, 8674–8690, <https://doi.org/10.1029/2018JD028447>, 2018.
- Yao, J., Liu, H., Huang, J., Gao, Z., Wang, G., Li, D., Yu, H., and Chen, X.: Accelerated dryland expansion regulates future variability in dryland gross primary production, *Nat. Commun.*, 11, 1665, <https://doi.org/10.1038/s41467-020-15515-2>, 2020.
- Yao, J., Gao, Z., Huang, J., Liu, H., and Wang, G.: US-Hn1 flux and meteorological data, figshare [data set], <https://doi.org/10.6084/m9.figshare.14747952>, 2021.
- Zeng, J., Matsunaga, T., Tan, Z. H., Saigusa, N., Shirai, T., Tang, Y., Peng, S., and Fukuda, Y.: Global terrestrial carbon fluxes of 1999–2019 estimated by upscaling eddy covariance data with a random forest, *Sci. Data*, 7, 1–11, <https://doi.org/10.1038/s41597-020-00653-5>, 2020.